Effect of an auxiliary acceptor on D–A––A sensitizers for highly efficient and stable dye-sensitized solar cells

Journal of Materials Chemistry A

ARTICLE

Effect of an Auxiliary Acceptor on D-A-π-A Sensitizers for Highly Efficient and Stable Dye-Sensitized Solar Cells

Received 00th January 20xx,
Accepted 00th January 20xx

DOI: 10.1039/x0xx00000x

www.rsc.org/

Yuting Gao,[a,b] Xing Li,[a] Yue Hu,[c,d] Yeli Fan,[b] Jianyong Yuan,[a] Neil Robertson,[d] Jianli Hua*[a] and Seth R. Marder*[b]

As one of the promising photovoltaic technologies, high performance metal-free dye-sensitized solar cells (DSSCs) have been explored due the fact that they can potentially produce using low-cost materials, their color can be tuned and they exhibit reasonable stability. Here three new organic donor–acceptor–π–acceptor (D-A-π-A) sensitizers (**B-87**, **Q-85** and **Q-93**), containing benzothiadiazole, two new modified pyrido[3,4-b]pyrazine as the auxiliary acceptor, have been synthesized and employed in DSSCs. Among the three dyes, **B-87** and **Q-85** showed good photovoltaic performance with power conversion efficiencies (PCE) up to 10.2% and 10.0%, respectively, which contribute to the few examples of DSSCs using pure organic dyes with iodine electrolyte to exceed the 10% efficiency barrier. It is noteworthy that an initial PCE of 7.16% has been achieved for **B-87** based DSSCs with ionic liquid electrolyte, which retained 95% of the initial efficiency after continuous light soaking for 1000 h at 60 °C, thus demonstrating outstanding stability. The molecular design strategy provides an effective approach to modulate the energy of the absorption bands as well as modify the optoelectronic and physical properties of the organic sensitizers to achieve highly efficient and stable sensitizers.

Introduction

As one of the promising photovoltaic technologies, dye-sensitized solar cells (DSSCs) have attracted considerable attention over the past 20 years.[1] A number of high power conversion efficiencies (PCEs) devices based on metal complexes dyes have been reported such as ruthenium[2] or porphyrin[3] complexes, reaching the highest PCE of 11-13%. However, ruthenium and porphyrin dyes suffer from either the resource scarcity and heavy metal toxicity or formidable synthesis. Therefore, the research activity has been increased in finding metal-free sensitizers with advantages of many aspects, such as facile synthetic approaches, high molar extinction coefficient within the visible region and tunable spectral properties.[4] Generally, most traditional organic sensitizers are synthesized with the donor–π–acceptor (D–π–A) configuration, making use of the efficient intramolecular charge transfer (ICT) process to harvest sunlight for photon-to-electron conversion.[5] From the viewpoint of stability and efficiency, Zhu et al. proposed a new concept of D–A–π–A motif by incorporating an additional group of electron-withdrawing conjugated components in 2011.[6] Based on this strategy, a series of D–A–π–A organic dyes incorporating internal electron-withdrawing units such as diketo-pyrrolo-pyrrole,[7] bithiazole,[8] isoindigo,[9] benzothiadiazole,[6, 10] benzotriazole,[11] and quinoxaline[12] into the traditional D–π–A structures were reported to modulate the energy levels, extend the spectral response and improve stability.

As noted above, the design of DSSCs molecular dyes requires careful consideration of multiple opto-electronic properties, such as band alignment and optical absorption coefficient, as well as solid-state properties such as dye aggregation, morphology, and mode of assembly on the TiO_2 photoanode. Zhu and co-workers performed extensive studies on 2,1,3-benzothiadiazole (BTD)-based sensitizers with this D–A–π–A motif, and the PCE of the DSSCs has been improved from 8.7% (WS-2)[6] to 9.0% (WS-9),[10] then to 10.08% (WS-51)[13] by changing different π-bridges to decrease the intermolecular interactions and retard the charge recombination. Inspired by their previous work, we substituted the cyclopenta[2,1-b:3,4-b']dithiophene (CPDT) with 4-bis (2-ethylhexyl)-4H-silolo[3,2-b:4,5-b']dithiophene (DTS) which is found to work very effectively on reducing dye aggregation as well as preventing charge recombination due to the presence of two out of plane 2-ethylhexyl.[14]

Pyrido[3,4-b]pyrazine (PP), an effective electron-withdrawing unit because of its two symmetric unsaturated nitrogen atoms and the pyridine N-atoms, has already been widely used and showed promising photovoltaic properties in photoelectric materials. However, its application as an auxiliary acceptor in DSSCs was seldom reported.[15] Hence, we introduced another

[a] Key Laboratory for Advanced Materials, Institute of Fine Chemicals, School of Chemistry and Molecular Engineering, East China University of Science and Technology, Shanghai 200237, People's Republic of China. E-mail: jlhua@ecust.edu.cn, Tel: (+) 86-21-64250940, Fax: (+) 86-21-64252758.
[b] School of Chemistry and Biochemistry and Center for Organic Photonics and Electronics, Georgia Institute of Technology, Atlanta, Georgia 30332-0400, United States. E-mail: seth.marder@chemistry.gatech.edu.
[c] Wuhan National Laboratory For Optoelectronics, Huazhong University of Science and Technology, 1037 Luoyu Road, Wuhan, Hubei Province 430074, People's Republic of China.
[d] School of Chemistry, University of Edinburgh, Edinburgh EH9 3FJ, UK
† Footnotes relating to the title and/or authors should appear here.
Electronic Supplementary Information (ESI) available: [details of any supplementary information available should be included here]. See DOI: 10.1039/x0xx00000x

two new modified PP-based acceptors other than BTD-based core as auxiliary acceptors to modulate the energy gap, expecting to broaden the spectral response. In addition, alkoxyl and alkyl chains were further introduced into the PP-based unit to suppress the dye aggregation and improve the solubility. As a result, three DTS-bridged D–A–π–A sensitizers with an alteration in auxiliary acceptors were rationally designed and exhibited excellent photovoltaic performances, with PCEs as high as 10.20% (**B-87**), 10.01% (**Q-85**) and 8.43% (**Q-93**), respectively. In this work, it will be seen that the change of auxiliary acceptors provides a useful strategy to modify the optoelectronic, chemical and physical properties of these organic sensitizers, thus generating high performance DSSCs.

Results and discussion

Molecular design and synthesis.

A coplanar and conjugated π-bridge unit DTS was inserted between the auxiliary acceptor and cyanoacrylic acid to facilitate charge transfer upon excitation from the ground to excited state and increase light absorption. Moreover, attaching two branched out of plane 2-ethylhexyl chains onto DTS appear to attenuate the interfacial recombination, for achieving better performance in devices. To further shift the absorption band to lower energy and enhance the ICT process, two modified PP-based cores with stronger electron-withdrawing ability were introduced into **Q-85** and **Q-93**, respectively (Fig. 1). With a more conjugated and electron withdrawing core, **Q-93** is to broaden and shift the absorption spectra the lower energy relative to **Q-85**.

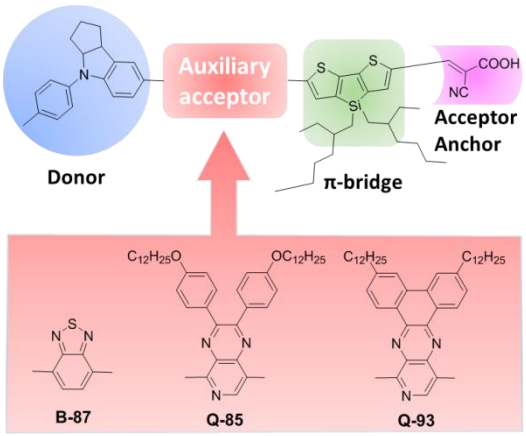

Fig. 1 Schematic representation of the D–A–π–A featured structures of **B-87**, **Q-85** and **Q-93** with different auxiliary acceptors.

The synthetic routes to **B-87**, **Q-85** and **Q-93** are depicted in Scheme 1. The intermediate compounds **3b-3c** were obtained according to literature.[16] Two sequential Suzuki coupling reactions with acceptors **3a-3b**, respectively, resulted in the corresponding aldehyde precursors **7b-7c** taking advantage of an in situ aldehyde deprotection.[14b] After deprotection of the aldehyde precursors, Knoevenagel condensation of compounds **8b-8c** with cyano acetic acid was conducted to give the target dyes **B-87**, **Q-85** and **Q-93** in 56%, 70% and 78% yields, respectively. Their structures were characterized by NMR, MS spectroscopies and EA (Fig. S5-S13, Electronic Supplementary Information (ESI)).

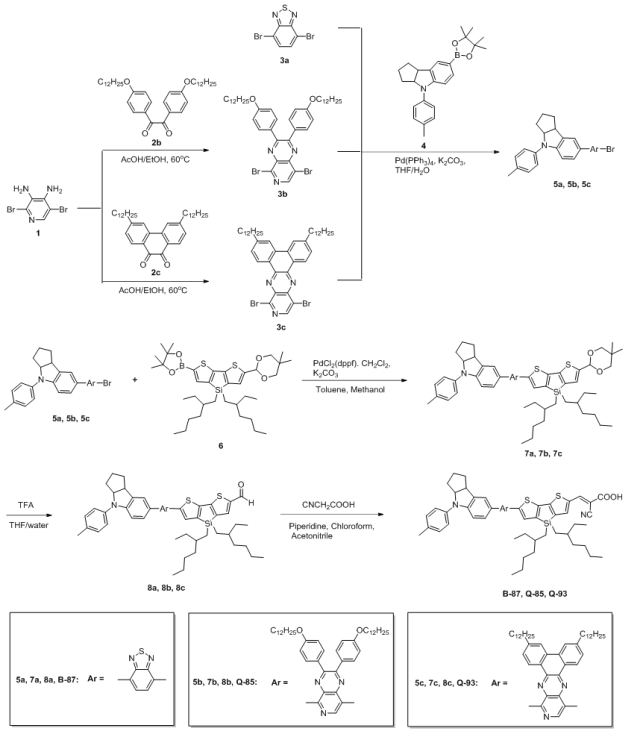

Scheme 1 Synthetic routes of dyes **B-87**, **Q-85** and **Q-93.**

Optical properties.

The UV-vis absorption spectra of **B-87**, **Q-85** and **Q-93** in CH_2Cl_2 solution and on TiO_2 films are shown in Fig. 2 and the corresponding data are summarized in Table 1. All of the three compounds exhibit three major electronic absorption bands: i) the electron transitions in UV region (around 300-350 nm), ii) the ICT band in visible region (around 560 nm for **B-87** and **Q-85**, 590 nm for **Q-93**), iii) the additional absorption band or shoulder from subordinate orbital transition (near 500 nm). Compared with the reported **WS-51** (λ_{max} = 551 nm),[13] the absorption maximum of **B-87** (λ_{max} = 562 nm) is 11 nm red-shifted along with a slight enhancement of molar extinction coefficient (ε) from 43000 to 47400 $M^{-1}cm^{-1}$. Interestingly, the two PP-based dyes, **Q-85** and **B-87** have similar band shapes with **B-87** showing an identical λ_{max} and an enhancement of ε to 50600 $M^{-1}cm^{-1}$ for the latter compoud. However, with a more coplanar and conjugated acceptor, λ_{max} of **Q-93** (593 nm, ε = 34600 $M^{-1}cm^{-1}$) is noticeably bathochromic-shifted by 31 nm compared to **B-87** and **Q-85**, which is related to the stronger withdrawing electron capability of the auxiliary acceptor. The tendency is consistent with the calculated optical gap and oscillator strength. As expected, the dye deprotonation and aggregation on TiO_2 film result in a shift and broadening of the absorption spectra that the maximum absorption peaks for **B-87**, **Q-85** and **Q-93** are blue-shifted to 543 nm, 543 nm and 586 nm, respectively.[13]

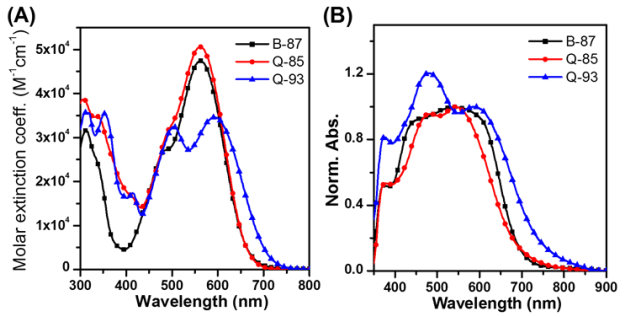

Fig. 2 Absorption spectra of **B-87**, **Q-85** and **Q-93** in CH_2Cl_2 solution (A) and adsorbed on TiO_2 transparent films (B).

Electrochemical data and DTF simulation.

To investigate the feasibility of electron injection from excited dyes into the conduction band of TiO_2 and dye regeneration by redox electrolyte, cyclic voltammetry (CV) measurements were performed in CH_2Cl_2 solution with ferrocene/ferrocenium (Fc/Fc^+) as an internal reference and 0.1 M tetra-n-butyl ammonium hexafluorophosphate as supporting electrolyte. As shown in Fig. 3, the position of $E_{S+/S}$ for **B-87**, **Q-85** and **Q-93** are located similarly at +0.94, +0.98 and +0.97 V *vs.* normal hydrogen electrode (NHE), respectively, which are estimated from the first oxidation potentials. These values suggest that all of the three sensitizers can provide ample driving force (almost 600 mV) for ground state regeneration of sensitizers, in consideration of I^-/I_3^- redox electrolyte (0.35 V *vs.* NHE).[17] The energy difference between the dye's excited state oxidation potential (E_{S+/S^*}) and the conduction band edge (E_{cb}) of TiO_2 (−0.5 V *vs.* NHE)[18] drives the electron injection from the photoexcited sensitizer to TiO_2. The driving force is estimated by substracting $E_{0\text{-}0}$ from $E_{S+/S}$, E_{S+/S^*} of dyes **B-87**, **Q-85** and **Q-93** are -1.06, -0.96 and -0.82 V *vs.* NHE, respectively, indicating sufficient thermodynamic force for electron injection.

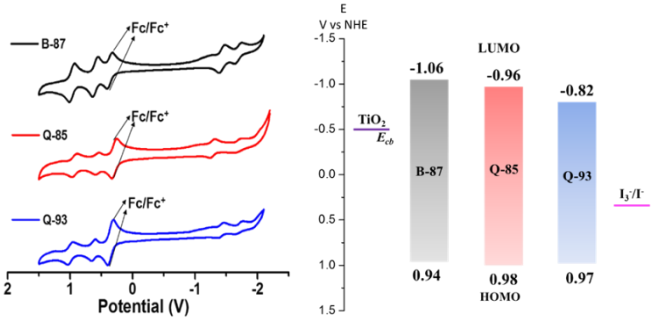

Fig. 3 The cyclic voltammograms of **B-87**, **Q-85** and **Q-93** with ferrocene/ferrocenium (Fc/Fc^+) as internal standard reference and energy diagram with respect to the conduction band of TiO_2.

In order to compare these experimental values and to gain further insight into structural properties, the frontier orbitals of the three compounds were calculated. (See ESI for details) The highest occupied molecular orbitals (HOMOs) and lowest unoccupied molecular orbitals (LUMOs) with their correspond-Ing energies (E_{HOMO} and E_{LUMO}) and the HOMO–LUMO gaps (ΔE) are depicted Table 2. It can be seen from Table S1 that the

Table 1 Optical properties and electrochemical properties of the dyes **B-87**, **Q-85** and **Q-93**.

Dye	λ_{max}[a] /nm	ε /M^{-1} cm^{-1}	$\lambda^{TiO2}{}_{max}$[b] /nm	$E_{S+/S}$[c] /V	$E_{0\text{-}0}$[d] /eV	E_{S+/S^*}[e] /V
B-87	562	47400	543	0.94	2.00	-1.06
Q-85	562	50600	543	0.98	1.94	-0.96
Q-93	593	34600	586	0.97	1.79	-0.82

[a] Absorption maximum in CH_2Cl_2 solution (2×10^{-6} M). [b] Absorption maximum on TiO_2 transparent films. [c] $E_{S+/S}$ was measured in CH_2Cl_2 with 0.1 M tetra-n-butylammonium hexafluorophosphate ($TBAPF_6$) as electrolyte which was calibrated with ferrocene/ferrocenium (Fc/Fc^+) as an internal reference and converted to a normal hydrogen electrode (NHE) by reference.[19] $E_{0\text{-}0}$ was determined from the intersection of the normalized absorption and emission spectra. [e] Calculated according to the following equation $E_{S+/S^*} = E_{S+/S} - E_{0\text{-}0}$

Table 2 Calculated charge transfer energies (E_{CT}, λ_{cal}), oscillator strengths (f) and corresponding experimental data (E_{exp}) of dyes[b].

Dyes	Crucial state	Contribution[a]	f	E_{CT}, λ_{cal}[b] eV(nm)	E_{exp}, λ_{exp} eV(nm)
B-87	S_1	H → L (70%) H → L+1 (18%)	1.93	2.20(564)	2.21(562)
	S_2	H→ L+1 (57%) H-1→ L (25%)	0.07	2.76(450)	2.53(490)
Q-85	S_1	H → L (54%) H-1 → L (27%)	1.98	2.21(560)	2.21(562)
	S_2	H-1 → L (26%) H → L+1 (54%)	0.06	2.69(461)	2.48(500)
Q-93	S_1	H → L (69%) H-1 → L (20%)	1.08	2.11(588)	2.09(593)
	S_2	H-1 → L (50%) H → L+1 (36%)	0.87	2.47(501)	2.51(495)

[a] H-1, H, L and L+1 represent HOMO-1, HOMO, LUMO and LUMO+1, respectively; the percentage contributions to wave functions of excited states are given in parentheses.
[b] Calculations are performed at the PCM(CH_2Cl_2)-LC-ωPBE/6-31G(d) level.

HOMO electrons in the three dyes are delocalized throughout the entire framework while the LUMOs are primarily distributed on the Acceptor-DTS-Anchor unit. This indicates that the configurations of the three dyes are highly conjugated with excellent electron transfer channels for electron injection. Meanwhile, such good overlap between the HOMO–LUMO orbital can facilitate the electron migration from donor to the anchor unit, then to the conduction band of semiconductor TiO_2. In addition, the HOMOs of the three dyes are almost the same, while the LUMOs follow the trend of **Q-93** (-2.85 eV) > **Q-85** (-2.93 eV) > **B-87** (-3.11 eV). The results are in good agreement with the experimental data, suggesting the corresponding electron withdrawing ability of the auxiliary acceptors, that is, **Q-93** > **Q-85** > **B-87**. Apart from that, the dihedral angle between the auxiliary acceptor and the π-bridge follows the order of **Q-93** (20.4°) > **Q-8**5 (17.4°) > **B-87** (-5.6°), as shown in

Table S2. The large dihedral angle may lead to a problem of electron transfer from the electron-rich donor to the auxiliary acceptor, illustrating that **Q-85** gives a similar absorption spectra with **B-87** even with a lower LUMO in CH_2Cl_2 solution. Furthermore, the larger twist in **Q-93** on both side of the auxiliary acceptor significantly decreases the oscillator strength of the lowest energy transition band, which corresponds to the relatively small extinction coefficient of the lowest energy band of **Q-93** from experimental. In constrast, the second lowest energy band, which is dominated by HOMO→LUMO+1 transition, has a much larger oscillator strength compared with the other two compounds, which can be attributed to the more planar geometry of the auxiliary acceptor in **Q-93**.

Photovoltaic performance.

The DSSCs performances of all the dyes were tested under AM 1.5G irradiation (1 sun, 100 mW cm^{-2}). Different layers of commercial colloidal paste was utilized to optimize the TiO_2 photoelectrode as shown in Fig. S2 and Table S3. With 12 µm thick commercial colloidal paste layer and 4 µm scattering layer TiO2 film, devices with all the three dyes showed best PCE. The photocurrent density voltage curves (*J-V*) and the incident photon to current conversion efficiency (IPCE) spectra of the optimized DSSCs based on dyes **B-87**, **Q-85** and **Q-93** are shown in Fig. 4. The detailed data of short-circuit current density (J_{sc}), open-circuit voltage (V_{oc}), fill factor (*FF*), and power conversion efficiency (PCE) are collected in Table 3. We now turn to the influence of altering the auxiliary acceptor core on the DSSCs characteristics. As we can see, both the J_{sc} and V_{oc} of the devices with **B-87**, **Q-85** and **Q-93** dyes decrease in the trend of **B-87** > **Q-85** > **Q-93**, and the PCEs of devices increase in order of **B-87** > **Q-85** > **Q-93**. The best PCE of 10.02% was obtained with **B-87** based on BTD core, possessing a typical J_{sc} of 20.28 mA cm^{-2}, a V_{oc} of 724 mV, and a fill factor of 68.26%. It is well known that the quantum conversion yield in response region and the spectrum coverage range determine the generation of photocurrent density. In this respect, we checked IPCE spectra to investigate the contribution of absorption at different wavelength to the J_{sc}, as shown in Fig. 4B. It can be clearly seen that the IPCE response are in the range of 300−805 nm for **B-87**, 300−750 nm for **Q-85** and 300−825 nm for **Q-93**, respectively. The onset wavelengths of photocurrent response from 300-350 nm are almost identical for the three dyes due to the same indoline donor. Interestingly, even though **B-87** and **Q-85** have almost the same absorption spectra in solution, **B-87** exhibited a more pronounced plateau in the IPCE response than **Q-85**, above 80% in the entire visible region of about 400-650 nm, presenting a higher current density of 20.28 mA cm^{-2}. Unsatisfactorily, the IPCE response for **Q-93** is the broadest but with the worst IPCE value that the plateau is no more than 75% from 400-700 nm, which is consistent with it having a lower molar extinction coefficient than **Q-85** , resulting a relatively low J_{sc} (19.53 mA cm^{-2}).

As to V_{oc}, the difference of the auxiliary acceptors in **B-87** and **Q-85** have little impact, which are 724 mV and 722 mV, respectively. Notably, there is a significant decline for **Q-93** (V_{oc}= 676 mV), with a more conjugated and coplanar electron-with-drawing core, compared with the other two dyes. Generally, the device's V_{oc} is influenced by the conduction band (E_{cb}) position and the recombination of electrons at the TiO_2/electrolyte interface.[20] To identify the position of TiO_2 conduction band, we fitted the cell chemical capacitance (C_μ) responses under a series of bias potentials, determined from the typical electrochemical impedance spectroscopy (EIS).[21] In these DSSCs with the three dyes, the logarithm of C_μ was enhanced at the almost identical slope with the given bias potential (Fig. 5A). We can see that the E_{cb} of the **B-87** and **Q-85** are similar, which is slightly higher than that of the **Q-93** device. This can be ascribed to the lower dipole moment of **Q-93**, shown in Table S2. As a dipole moment pointing away from the TiO_2 surface will cause an increase in the energy splitting between the quasi-Fermi level for electrons in the TiO_2 and that for holes in the redox couple, which results in a larger V_{oc}.[22]

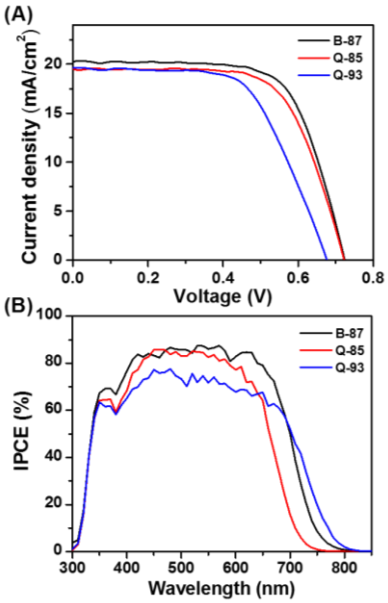

Fig. 4 (A) *J-V* curves for DSSCs based on the dyes under illumination of AM 1.5 G simulated sunlight (100 mW cm^{-2}). (B) IPCE spectra of the same DSSCs.

Table 3. Photovoltaic performance of the DSSCs based on **B-87**, **Q-85** and **Q-93**[a].

Dye	V_{oc} (mV)	J_{sc} (mA cm^{-2})	*FF* (%)	PCE (%)
B-87	724	20.28	68.26	10.02
Q-85	722	19.55	66.64	9.41
Q-93	676	19.53	61.83	8.17

[a]Measured under irradiation of AM 1.5 simulated solar light (100 mW cm^{-2}) at room temperature, iodide electrolyte was utilized containing: 1.0 M 1, 3-dimethylimidazolium iodide, 0.03 M iodine, 0.1 M guanidinium thiocyanate, 0.5 M tert-butylpyridine, 0.05 M lithium iodide in acetonitrile:valeronitrile (85:15, v/v), the concentration of dyes is 3 × 10^{-4} M in chloroform/ethanol (v/v: 4/6) mixed solvent, platinum is the counter electrode.

In addition, we can see clearly that **B-87**–based DSSCs exhibited a slight increase of the charge-transfer resistance (R_{ct}) under a series of bias potentials in comparison to **Q-85**, whereas, there was an obvious increase compared with **Q-93**, which can be attributed to less charge recombination of **Q-93**-DSSCs. The data suggest that relatively subtle structural difference on the central electron-deficient unit among the three dyes can result in a significant difference in the rate charge recombination (**B-87** > **Q-85** > **Q-93**), which may be attribute to the aggregation and electron-withdrawing ability. The stronger electron-withdrawing ability of PP-based core could increase the probability of electron recombination from TiO_2 to oxidized dyes thus lead to a lower V_{oc} value for the PP-based DSSCs.

The electron lifetime (τ_n=C_{chem}×R_{ct}) versus the chemical capacitance is also plotted for all the devices to further compare the differences in the electron recombination processes (shown in Fig. 5C).[21a, 23] The longer the electron lifetime in titania films, should lead to a higher the electron density and thus higher pseudo-Fermi level, which might result in higher V_{oc}. The electron lifetime of **B-87** device is the longest under certain bias potential, followed in descending order by **Q-85** and **Q-93** devices. The results further illustrate that **B-87** with BTD core displays better performance in retarding the electron recombination process than the PP core of **Q-85** and **Q-93**. Moreover, the dark currents under different bias potential in DSSCs based on **B-87**, **Q-85** and **Q-93** were presented in Fig. 5D. The smaller dark current in DSSCs based on **B-87** suggests less charge recombination between TiO_2 surface and electrolyte, and less loss of current in device,[24] which can partly explain the higher J_{sc} and V_{oc} of DSSC based on **B-87** than **Q-85** and **Q-93**.

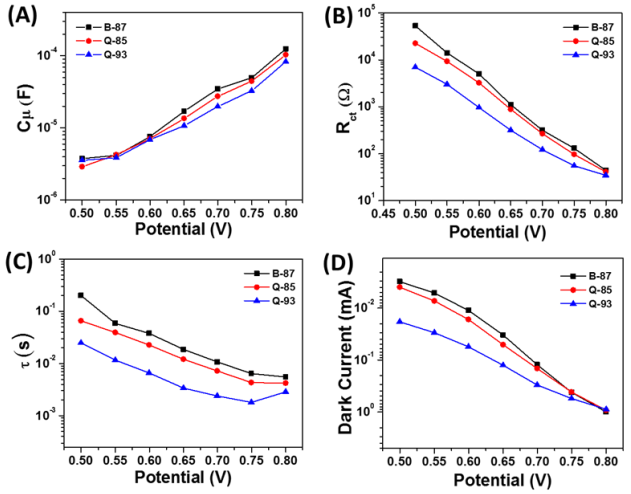

Fig. 5 Plots of cell capacitance C_μ (A), interface charge transfer resistance R_{ct} (B), calculated electron lifetime τ_n (C) and dark current (D) under a series potential bias of DSSCs based on sensitizers **B-87**, **Q-85** and **Q-93** (dye bath solvent: $CHCl_3$:C_2H_5OH, v/v= 6:4, dipping time: 12 h)

Inspired by previous work, utilization of a coadsorbent is an effective approach for suppressing dye aggregation, thus enhancing V_{oc}. Given the relatively low V_{oc} values of the three dyes, Chenodeoxycholic acid (CDCA), a commonly used coadsorbent due to its nonplanar and bulky configuration, was used for the consequent optimization. Initially, DSSCs were fabricated by dipping the TiO_2 films into the dye solutions containing concentration of CDCA. The optimized process and data of CDCA concentration are shown in Fig. S3 and Table S4. The result showed that a concentration of 6 mM CDCA is the best condition for the B-87-based DSSCs. The *J-V* curves of DSSCs coadsorbing with 6 mM CDCA were given in Fig. 6A and the corresponding photoelectric results were tabulated in Table 4. Unexpectedly, the PCE for **B-87**-based DSSC improved from 10.02% to 10.20%, however, an undesirable decrease was observed in PP-based dyes of **Q-85** and **Q-93** from 9.41% and 8.17% to 7.31% and 7.35%, respectively. The 20.78 mA cm^{-2} achieved for **B-87** coadsorbed with CDCA is slightly higher than previous 20.28 mA cm^{-2}, which can account for the improvement of PCE with V_{oc} remaining the same. As shown in Fig. 6C, a narrower but higher IPCE response of **B-87** devices with CDCA suggests that the aggregation was indeed repressed, thus resulting in more efficient charge transport and collection, which could explain the increase of J_{sc}.[25] In contrast with **B-87**, it is odd to see the synchronous decline in both J_{sc} and V_{oc} for **Q-85** and **Q-93**-based DSSCs. During the optimization procedure, it was observed that the TiO_2 films soaking in PP-based dye bath (3×10^{-4} M), **Q-85** and **Q-93**, with 6 mM CDCA for 12 h were less intensely colored than those prepared with pure dyes, as shown in Fig. 7. This phenomenon is not seen for **B-87**-based dyes, suggesting that competitive adsorption between PP-based dyes with CDCA is more predominate than BT-based dyes. To probe our hypothesis, the extent of dye adsorption for the corresponding DSSC devices were measured by the desorption method and the data is summarized in Table 4. The results confirm that the dye-loading amounts of PP-based dyes were reduced significantly, wherein **Q-85** decreased from 1.21×10^{-7} to 5.83×10^{-8} mol cm^2 and **Q-93** decreased from 1.20×10^{-7} to 8.50×10^{-8} mol cm^2, upon the coadsorption with CDCA. Whereas the dye-loading amount of **B-87** did not change significantly, showing a slight decline from 1.32×10^{-7} to 1.13×10^{-7} mol cm^2. One plausible explanation for this phenomenon is that the N atom of pyridine ring in PP unit could decrease the pKa value of CDCA, thus increasing the bonding ability of CDCA with TiO_2, however further experimentation would need to be performed to confirm this.

Considering the detrimental result of simultaneous coadsorption of **Q-85** and **Q-93** along with CDCA, an alternative coadsorption method was performed to lessen the competitive effect of CDCA. Herein, we dipped the TiO_2 films into 6 mM CDCA solution in ethanol for 30 min, then in dyes solution for 12 h after been washed and dried. As a result, even though there was no enhancement of PCE for **B-87**-based DSSC, the PCE for **Q-85** and **Q-93**-based DSSCs was strikingly improved from 9.41% and 8.14% to 10.01% and 8.43%, respectively (Fig. 6B and Table 4). As anticipated, the V_{oc} of **Q-85** and **Q-93**-based DSSCs were significantly enhanced, which might be attributed to suppression of aggregation of the dyes. The decreased J_{sc} of the devices may be related to the decreased coverage of dyes, leading to a loss in light harvesting process. The downward IPCE curves shown in Fig. 6D and 6E could also account for the decrease of J_{sc}, compared with pure dyes.

Table 4 Photovoltaic performance of the DSSCs based on **B-87**, **Q-85** and **Q-93** with CDCA as a coadsorbent.

Dye	CDCA[a, b]	Adsorption amount (mol cm^2)	V_{oc} (mV)	J_{sc} (mA cm^{-2})	*FF* (%)	PCE (%)
B-87	0	1.32×10^{-7}	724	20.28	68.26	10.02
	6 mM[a]	1.13×10^{-7}	724	20.78	67.77	10.20
	6 mM[b]	9.72×10^{-8}	694	20.17	70.69	9.90
Q-85	0	1.21×10^{-7}	722	19.55	66.64	9.41
	6 mM[a]	5.83×10^{-8}	682	15.74	68.08	7.31
	6 mM[b]	1.03×10^{-7}	738	19.54	69.42	10.01
Q-93	0	1.20×10^{-7}	676	19.53	61.83	8.17
	6 mM[a]	8.50×10^{-8}	638	15.83	72.67	7.35
	6 mM[b]	1.11×10^{-7}	694	18.89	64.33	8.43

[a] The films were dipped in a solution ($CHCl_3$:C_2H_5OH, v/v= 6:4) with dyes (3×10^{-4} M) and CDCA (6×10^{-3} M) for 12 h. [b] The films were dipped in CDCA ethanol solution for 30 min first, then dipped in dye baths with a concentration of 3×10^{-4} M ($CHCl_3$:C_2H_5OH, v/v= 6:4) for 12 h.

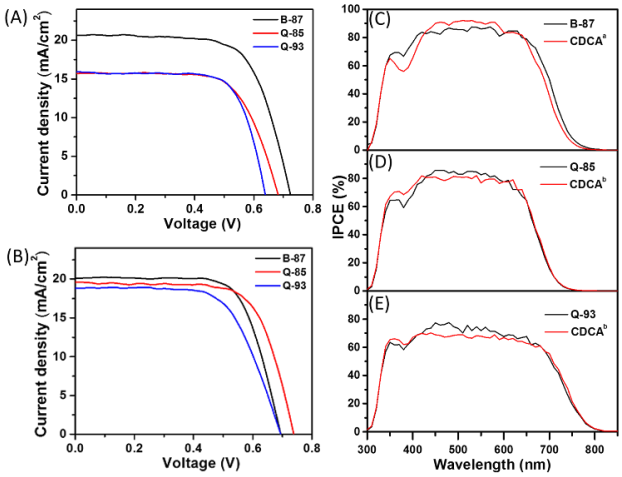

Fig. 6 *J-V* curves for DSSCs under illumination of AM 1.5 G simulated sunlight (100 mW cm^{-2}) with coadsorption of CDCA by two methods, (A) dipping in a solution ($CHCl_3$:C_2H_5OH,v/v= 6:4) with dyes and CDCA for 12 h. (B) dipping in CDCA ethanol solution for 30 min first, then dipping in dyes bath ($CHCl_3$:C_2H_5OH,v/v= 6:4) for 12 h. (C) IPCE spectra of DSSCs dipping in dye bath of pure **B-87** and coadsorbing with CDCA in method a, respectively. (D) IPCE spectra of DSSCs dipping in dye bath of pure **Q-85** and coadsorbing with CDCA in method b, respectively. (E) IPCE spectra of DSSCs dipping in dye bath of pure **Q-93** and coadsorbing with CDCA in method b, respectively.

To further study the impact of the coadsorbing CDCA on V_{oc}, the EIS analysis was also performed. Fig. 8 depicts the C_μ and R_{ct} of **B-87**, **Q-85** and **Q-93** with and without CDCA under a series bias potential. We can see that no relative shifts of conduction band in TiO_2 were observed in presence with CDCA on account of the similar C_μ values with pure dyes. In other words, the values of V_{oc} are directly correlated with the electron density in TiO_2. Compared with pure dyes-based DSSCs, R_{ct} values of the coadsorbing DSSCs are larger than pure dyes at fixed potential, suggesting the inhibition of the interfacial electron recombination process.[26] (Fig. 8), which suggests less charge recombination in presence of CDCA. As a consequence, the combined effect gives the larger τ_{CDCA} than pure dyes, illustrating the relatively higher V_{oc}.

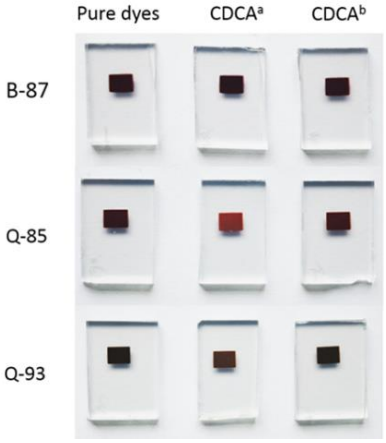

Fig. 7 The pictures of **B-87**, **Q-85** and **Q-93** adsorbed on TiO_2 films in different conditions before fabricated into DSSCs. CDCA[a] means dipping in a solution ($CHCl_3$:C_2H_5OH, v/v= 6:4) with dyes (3×10^{-4} M) and CDCA (6×10^{-3} M) for 12 h. CDCA[b] means dipping in CDCA ethanol solution for 30 min first, then dipping in dye baths with a concentration of 3×10^{-4} M ($CHCl_3$:C_2H_5OH, v/v= 6:4) for 12 h.

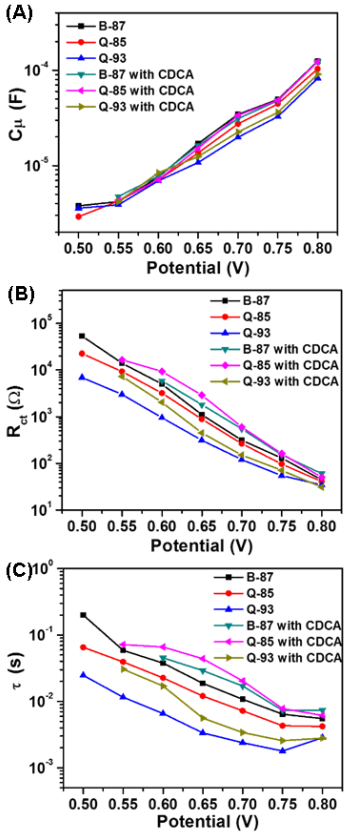

Fig. 8 Plots of cell capacitance C_μ (A), interface charge transfer resistance R_{ct} (B), calculated electron lifetime τ (C) under a series potential bias of DSSCs based on pure dyes and their coadsorption with CDCA (**B-87** with CDCA in method a, **Q-85** and **Q-93** with CDCA in method b).

Stability Measurements.

In addition to high PCE, long-term stability is a vital requirement for the practical application of dye-sensitized solar cells. Compared with liquid electrolyte, the solvent-free ionic liquid electrolytes have been shown in DSSCs with excellent long-term device stability. Possessing the highest PCE of DSSCs based on the three dyes, **B-87** was chosen to optimize the DSSCs performance with ionic liquid electrolyte which contains 1,3-dimethylimidazoliumiodide / 1-ethyl-3 methylimidazoliumio-dide / 1-ethyl-3-methyl-imidazolium tetracyanoborate / iodine / Nbutylbenzoimidazole / guanidinium thiocyanate (molar ratio 12 / 12 / 16 / 1.67 / 3.33 / 0.67). Different thickness of the photoelectrode was fabricated by repeating screen printing process with different layers of commercial colloidal paste. The *J-V* curves of corresponding DSSCs under standard AM 1.5G full sunlight conditions were given in Fig. S4 and their photoelectric results were summarized in Table 5. With 8 μm thick commercial colloidal paste layer and 4 μm scattering layer TiO_2 film, devices with **B-87** showed best PCE of 7.16% with J_{sc} of 16.59 mA/cm^2, V_{oc} of 699 mV and *FF* of 69%. The decreased J_{sc} of device with thicker TiO_2 layer (12+4) could be ascribed to the poor contact between dyes and ionic liquid electrolyte and lower diffusion rate, which can affect the dye regeneration. The devices were subjected to long-term stability tests under the irradiance of AM 1.5G full sun visible light soaking at 60 °C. The detailed photovoltaic parameters of devices during the aging process are presented in Fig. 9. It can be seen that the PCE of the DSSCs increases significantly in the beginning, which is related to the improved penetration of the ionic liquid electrolyte through the complete thickness of the electrode and the ''activation'' of the entire electrode.[27] After that a stabilization of the performances was observed and the PCE of the devices remained at 95% of the initial value under both the thermal and the light-soaking stress for over 1000 h, showing outstanding stability.

Table 5 Photovoltaic performance of the DSSCs based on **B-87**[a].

TiO_2 Thickness[b] (μm)	V_{oc} (mV)	J_{sc} (mA cm^{-2})	*FF* (%)	PCE (%)
4 + 4	712	14.48	64.12	6.61
8 + 4	699	16.59	61.74	7.16
12 + 4	619	15.14	71.61	6.71

[a]Measured under irradiation of AM 1.5 simulated solar light (100 mW cm^{-2}) at room temperature, the concentration of dyes is 3 × 10^{-4} M in chloroform/ethanol (v/v: 4/6) mixed solvent (dipping time: 12h). [b]Thick commercial colloidal paste TiO_2 film layer + scattering TiO_2 film layer.

Conclusions

In summary, three DTS-bridged D−A−π−A sensitizers with a variation in auxiliary acceptors were synthesized and each exhibited excellent photovoltaic performances, with PCE as high as 10.0% (**B-87**), 9.4% (**Q-85**) and 8.2% (**Q-93**), respectively, in

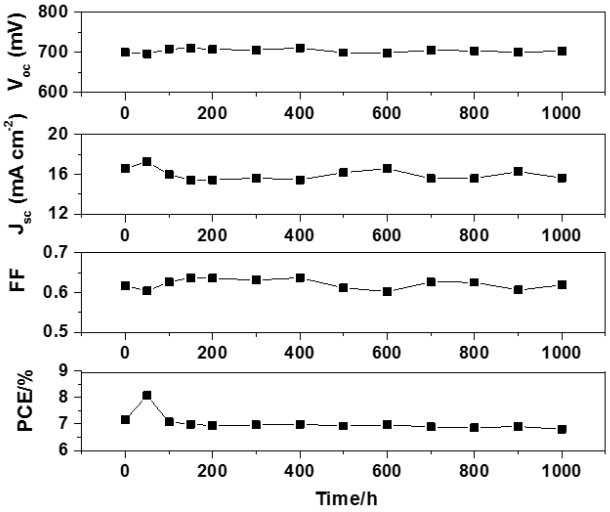

Fig. 9 Detailed photovoltaic parameters of **B-87** based DSSC with (8+4) μm TiO_2 Thickness measured under irradiation of AM 1.5 simulated solar light (100 mW cm^{-2}) at 60 °C. (Ionic liquid electrolyte).

standard I_3^-/I^- liquid electrolyte. The relationship between the molecular structure and the photovoltaic performance of the dye cells were examined using *J-V* scan, IPCE and EIS. The substitution of CPDT bridge with DTS in **B-87** results in a red-shift of absorption spectra and enhanced molar extinction coefficient compared with the reported **W-51**. Compared with **B-87** and **Q-85**, **Q-93** with broader absorption band showed unsatisfactory PCE owing to a lower IPCE and shorter electron lifetime. After coadsorption with CDCA in two different methods, the photovoltaic performances of the three dyes have been improved obviously, achieving PCE of 10.20% (**B-87**), 10.01% (**Q-85**) and 8.43% (**Q-93**), respectively. Furthermore, the stability of **B-87** based DSSCs with ionic liquid electrolyte was evaluated. After optimization of the photoelectrode, a PCE of up to 7.16 % has been achieved for **B-87** based DSSCs with ionic-liquid electrolytes, which retained 95% of the initial performances after continuous light soaking for 1000 h at 60°C. This work demonstrates the potential application of **B-87** dyes as a promising candidate for highly efficient and stable DSSCs devices.

Experimental section

Materials and reagents. Fluorine-doped SnO_2 conducting glass (FTO glass, transparency > 90%, sheet resistance 15 Ω/square was obtained from the Geao Science and Educational Co. Ltd. of China. Acetonitrile, tetra-n-butyl ammonium hexafluorophos-phate ($TBAPF_6$), 4-tert-butylpyridine, and lithium iodide were bought from Fluka and iodine (99.999%) was purchased from Alfa Aesar. Transparent TiO_2 paste (18NR-T) was purchased from Dyesol Ltd. Light-scattering anatase particles were obtained from the Shanghai Institute of Ceramics. Tetrahydrofuran (THF) was pre-dried over 4 Å molecular sieves and distilled under argon atmosphere from sodium benzophenone ketyl immediately prior to use. Triethylamine

was distillated under normal pressure and dried over potassium hydroxide. *N, N*-dimethyl formamide (DMF), dichloromethane (DCM) and chloroform were reflux with calcium hydride and distilled before used. The starting materials and intermediates **1**,[28] **2b**,[16a] **2c**,[29] **4**[30] and **6**[14a] were prepared according to published procedures. All other chemicals were purchased from Aldrich and used as received without further purification.

Instruments and characterization. Chromatographic separations were performed using standard flash column chromatography methods using silica gel purchased from Sorbent Technologies (60 Å, 32-63 μm). A Brücker AMX-400 spectrometer was employed to obtain ^{1}H NMR and ^{13}C NMR spectra with TMS as the internal standard. Mass spectra were recorded on an Applied Biosystems 4700 Proteomics Analyzer at the Mass Spectrometry Facility at the Georgia Institute of Technology. Elemental analyses were performed by Atlantic Microlabs. UV-Vis-NIR spectra were recorded in 1 cm quartz cuvette using a Varian Cary 5E spectrometer. Electrochemical measurements were carried out under nitrogen in dry deoxygenated 0.1 M tetra-n-butylammonium hexafluorophosphate in dichloromethane (ca. 10^{-4} M of analyte) using conventional three-electrode cell with a glassy carbon working electrode, platinum wire counter electrode, and a Ag wire coated with AgCl as pseudo-reference electrode. Potentials were referenced to ferrocenium/ferrocene. Cyclic voltammograms were recorded at a scan rate of 50 mV/s.

Synthesis of sensitizers. *5,8-dibromo-2,3-bis(4-(dodecyloxy)-phenyl)pyrido[3,4-b]pyrazine (**3b**)*: A solution of **1** (0.67 mg, 2.5 mmol) and **2b** (1.45 g, 2.5 mmol) in 35 ml ethanol was added acetic acid (15.0 mL). The reaction mixture was heated and kept reflux for 6 h. The mixture was cooled to room temperature. The reaction mixture was poured into water (150.0 mL). The yellow solid was collected with filtration and washed with water. After dried, the crude product was purified on a silica gel column using hexanes /dichloromethane (volume = 2:1) as the elutant to afford pure product **3b** as a yellow powder (676 mg, yield: 61%). ^{1}H NMR (400 MHz, $CDCl_3$) δ 8.68 (s, 1H), 7.67 (dd, *J* = 10.8, 8.8 Hz, 4H), 6.89 (dd, *J* = 8.8, 2.4 Hz, 4H), 4.00 (t, *J* = 6.5 Hz, 4H), 1.88 – 1.74 (m, 4H), 1.52 – 1.40 (m, 4H), 1.39 – 1.15 (m, 32H), 0.88 (t, *J* = 6.8 Hz, 6H). ^{13}C NMR (101 MHz, $CDCl_3$) δ 161.29, 160.96, 157.66, 155.57, 146.66, 145.80, 142.14, 135.61, 131.94, 131.68, 129.67, 129.49, 119.96, 114.53, 68.21, 68.19, 31.93, 29.68, 29.65, 29.62, 29.59, 29.41, 29.37, 29.19, 29.17, 26.03, 22.71, 14.14. HRMS (MALDI) *m/z*: $[M+H]^+$ calcd. for $C_{43}H_{59}Br_2N_3O_2$: 808.2974; found, 808.3014. Anal. Calcd. for $C_{43}H_{59}Br_2N_3O_2$: C, 63.78; H, 7.34; N, 5.09. Found: C, 63.97; H, 7.19; N, 5.03.

*10,13-dibromo-3,6-didodecyldibenzo[f,h]pyrido[3,4-b]quinoxaline (**3c**):* A solution of **1** (0.80 mg, 3.0 mmol) and **2c** (1.09 g, 2.0 mmol) in 30.0 mL ethanol was added acetic acid (10.0 ml). The reaction mixture was heated and kept reflux for 6 h. The mixture was cooled to room temperature. The reaction mixture was poured into water (150.0 mL). The yellow solid was collected with filtration and washed with water. After drying, the crude product was purified on a silica gel column using hexanes /dichloromethane (5:3) as the eluant to afford pure product **3c** as a yellow powder (1.4 g, yield: 90%). ^{1}H NMR (400 MHz, $CDCl_3$) δ 9.20 (t, *J* = 7.6 Hz, 2H), 8.78 (d, *J* = 0.5 Hz, 1H), 8.26 (s, 2H), 7.56 (dd, *J* = 4.0 Hz, *J* = 8.2 Hz, 2H), 2.92 (t, *J* = 7.6 Hz, 4H), 1.86 – 1.78 (m, 4H), 1.49 – 1.28 (m, 36H), 0.90 (t, *J* = 6.8 Hz, 6H). ^{13}C NMR (101 MHz, $CDCl_3$) δ 147.87, 147.23, 146.81, 146.44, 145.65, 144.75, 142.23, 136.05, 133.15, 132.41, 129.04, 128.95, 127.68, 127.22, 126.63, 126.38, 122.52, 122.45, 120.35, 36.77, 36.72, 31.94, 31.54, 31.51, 29.71, 29.68, 29.61, 29.49, 29.38, 22.71, 14.14. HRMS (MALDI) *m/z*: $[M+H]^+$ calcd. for $C_{43}H_{57}Br_2N_3$: 774.2919; found, 774.3005. Anal. Calcd. for $C_{43}H_{57}Br_2N_3$: C, 66.58; H, 7.41; N, 5.42. Found: C, 66.28; H, 7.16; N, 5.36.

*4-bromo-7-(4-(p-tolyl)-1,2,3,3a,4,8b-hexahydrocyclopenta[b]indol-7-yl)benzo[c][1,2,5]thiadiazole (**5a**):* Under an argon atmosphere, a mixture of **3a** (1.18 g, 4.0 mmol) and $Pd(PPh_3)_4$ (231 mg, 0.2 mmol) in THF (30 mL) was heated to 60 °C, then 10 mL of 2 M K_2CO_3 aqueous solution was added, followed by injecting a solution of **4** (1.24 g, 3.3 mmol) in 10 mL THF slowly. Then the mixture was heated to refluxed for 8 h. After it was cooled, 150 mL water was added to quench to reaction and the raw product was extracted using CH_2Cl_2 and water. The organic layers were combined and dried by anhydrous Na_2SO_4. After filtration, the solvent was removed under reduced pressure, and the residue was purified by chromatography on a silica gel column with hexanes /dichloromethane (volume = 6:1) to give **5a** as red solid (810 mg, yield: 53%). ^{1}H NMR (400 MHz, $CDCl_3$) δ 7.86 (d, *J* = 7.6 Hz, 1H), 7.70 (s, 1H), 7.65 (d, *J* = 8.4 Hz, 1H), 7.51 (d, *J* = 7.6 Hz, 1H), 7.24 (d, *J* = 8.3 Hz, 2H), 7.18 (d, *J* = 8.2 Hz, 2H), 7.00 (d, *J* = 8.3 Hz, 1H), 4.87 (t, *J* = 7.0 Hz, 1H), 3.93 (t, *J* = 8.2 Hz, 1H), 2.35 (s, 3H), 2.17 – 2.04 (m, 1H), 2.00 – 1.90 (m, 2H), 1.87 – 1.75 (m, 1H), 1.73 – 1.56 (m, 2H). ^{13}C NMR (101 MHz, $CDCl_3$) δ 153.99, 153.37, 148.77, 140.01, 135.45, 134.49, 132.48, 131.88, 129.84, 128.88, 126.37, 126.34, 125.50, 120.45, 110.88, 107.35, 69.32, 45.39, 35.23, 33.69, 24.46, 20.85. HRMS (ESI) *m/z*: $[M+H]^+$ calcd. for $C_{24}H_{21}BrN_3S$: 462.0640; found, 462.0638.

*7-(8-bromo-2,3-bis(4-(dodecyloxy)phenyl)pyrido[3,4-b]pyrazin-5-yl)-4-(p-tolyl)-1,2,3,3a,4,8b-hexahydrocyclopenta[b] (**5b**):* Under an argon atmosphere, a mixture of **3b** (1.6 g, 2 mmol) and $Pd(PPh_3)_4$ (116.0 mg, 0.1 mmol) in THF (20 mL) was heated to 60 °C, then 5 mL of 2 M K_2CO_3 aqueous solution was added, followed by injecting a solution of **4** (626.7 mg, 1.67 mmol) in THF slowly. Then the mixture was heated to refluxed for 8 h. After it was cooled, 50 mL water was added to quench to reaction and the raw product was extracted using CH_2Cl_2 and water. The organic layers were combined and dried by anhydrous Na_2SO_4. After filtration, the solvent was removed under reduced pressure, and the residue was purified by chromatography on a silica gel column with hexanes /dichloromethane (volume = 2:1) to give **5b** as red solid (810 mg, yield: 50%). ^{1}H NMR (400 MHz, $CDCl_3$) δ 8.93 (s, 1H), 8.15 (s, 1H), 8.10 (dd, *J* = 8.5, 1.7 Hz, 1H), 7.75 (d, *J* = 8.8 Hz, 1H), 7.63 (d, *J* = 8.8 Hz, 2H), 7.28 (d, *J* = 8.4 Hz, 2H), 7.22 (d, *J* = 8.4 Hz, 2H), 7.03

(d, *J* = 8.5 Hz, 1H), 6.89 (dd, *J* = 18.3, 8.8 Hz, 4H), 5.18 – 4.77 (m, 1H), 4.14 – 3.82 (m, 5H), 2.39 (s, 3H), 2.21 – 2.04 (m, 2H), 2.02 – 1.92 (m, 1H), 1.90 – 1.77 (m, 5H), 1.77 – 1.60 (m, 2H), 1.55 – 1.42 (m, 4H), 1.40 – 1.23 (m, 32H), 0.90 (dt, *J* = 6.9, 3.3 Hz, 6H). ^{13}C NMR (101 MHz, $CDCl_3$) δ 160.87, 160.30, 158.41, 155.43, 152.79, 149.60, 147.42, 141.73, 139.93, 134.67, 131.96, 131.83, 131.47, 130.67, 130.21, 129.86, 127.92, 127.25, 120.68, 115.97, 114.43, 114.34, 106.84, 69.38, 68.16, 68.13, 45.39, 35.22, 33.68, 31.99, 29.71, 29.67, 29.66, 29.48, 29.42, 29.26, 26.10, 24.51, 22.76, 20.90, 14.20. HRMS (MALDI) *m/z*: $[M]^+$ calcd. for $C_{61}H_{77}BrN_4O_2$: 976.5230; found, 976.5263. Anal. Calcd. for $C_{61}H_{77}BrN_4O_2$: C, 74.90; H, 7.93; N, 5.73. Found: C, 75.17; H, 7.93; N, 5.60.

*13-bromo-3,6-didodecyl-10-(4-(p-tolyl)-1,2,3,3a,4,8b-hexahydrocyclopenta[b]indol-7-yl)dibenzo[f,h]pyrido[3,4-b]quinoxaline(**5c**):* Under an argon atmosphere, a mixture of **3c** (1.60 g, 2.06 mmol) and $Pd(PPh_3)_4$ (92.4 mg, 0.08 mmol) in THF (20 mL) was heated to 60 °C, then 5 mL of 2 M K_2CO_3 aqueous solution was added, followed by injecting a solution of **4** (1.58 mmol, 593.0 mg) in THF slowly. Then the mixture was heated to refluxed for 8 h. After it was cooled, 50 mL water was added to quench to reaction and the raw product was extracted using CH_2Cl_2 and water. The organic layers were combined and dried by anhydrous Na_2SO_4. After filtration, the solvent was removed under reduced pressure, and the residue was purified by chromatography on a silica gel column with hexanes /dichloromethane (volume = 2.4 : 1) to give **5c** as dark red solid (850 mg, yield: 57%). ^{1}H NMR (400 MHz, $CDCl_3$) δ 9.39 (d, *J* = 8.2 Hz, 1H), 9.11 (d, *J* = 8.2 Hz, 1H), 9.05 (s, 1H), 8.35 (s, 2H), 8.29 – 8.21 (m, 2H), 7.62 (dd, *J* = 8.3, 1.2 Hz, 1H), 7.55 (dd, *J* = 8.2, 1.3 Hz, 1H), 7.38 – 7.30 (m, 2H), 7.25 (d, *J* = 8.3 Hz, 2H), 7.12 (d, *J* = 8.4 Hz, 1H), 5.03 – 4.88 (m, 1H), 4.09 – 3.86 (m, 1H), 2.93 (2t, *J* = 7.6, 7.6 Hz, 4H), 2.40 (s, 3H), 2.25 – 2.11 (m, 2H), 2.10 – 1.94 (m, 1H), 1.94 – 1.66 (m, 7H), 1.52 – 1.20 (m, 36H), 0.95 – 0.83 (m, 6H). ^{13}C NMR (101 MHz, $CDCl_3$) δ 159.36, 159.34, 149.62, 146.98, 146.76, 146.08, 144.91, 142.93, 142.43, 139.94, 136.05, 134.67, 132.90, 132.26, 132.02, 129.89, 128.80, 128.67, 128.29, 127.71, 127.66, 127.38, 127.24, 126.98, 122.50, 122.46, 120.72, 116.38, 106.87, 69.41, 45.47, 36.74, 36.67, 35.22, 33.74, 31.94, 31.65, 31.57, 29.72, 29.68, 29.62, 29.53, 29.49, 29.39, 24.56, 22.71, 20.90, 14.14. HRMS (MALDI) m/z: [M]+ calcd. for $C_{61}H_{75}BrN_4$: 942.5179; found, 942.5199. Anal. Calcd. for $C_{61}H_{75}BrN_4$: C, 77.60; H, 8.01; N, 5.93. Found: C, 77.34; H, 7.89; N, 5.85.

*4-(6-(5,5-dimethyl-1,3-dioxan-2-yl)-4,4-bis(2-ethylhexyl)-4H-silolo[3,2-b:4,5-b']dithiophen-2-yl)-7-(4-(p-tolyl)-1,2,3,3a,4,8b-hexahydrocyclopenta[b]indol-7-yl)benzo[c][1,2,5]thiadiazole (**7a**):* Compound **5a** (231.2 mg, 0.5 mmol), compound **6** (658.9 mg, 1.0 mmol), [1,1'bis(diphenylphosphino)ferrocene] dichloro palladium(II) (36.6 mg, 0.05 mmol) and potassium carbonate (345 mg, 2.5 mmol) were placed in a dry two-neck round bottom flask. Under nitrogen, methanol (5.0 mL) and anhydrous toluene (20 mL) were added and the reaction mixture was subjected to three freeze/pump/thaw cycles after which the reaction flask was refilled with nitrogen. The solution was heated to 80 °C for 12 hours. The solvents were removed under reduced pressure and the crude product was extracted using DCM and water. The DCM extract was filtered through Celite® and then passed through a column of silica eluting with hexanes /DCM (volume = 3:1) to get purple solid (405 mg, yield: 88%).^{1}H NMR (400 MHz, $CDCl_3$) δ 8.14 (t, *J* = 5.5 Hz, 1H), 7.90 (d, *J* = 7.6 Hz, 1H), 7.80 (s, 1H), 7.75 (dd, *J* = 8.3, 1.7 Hz, 1H), 7.68 (d, *J* = 7.6 Hz, 1H), 7.27 (d, *J* = 9.2 Hz, 2H), 7.20 (d, *J* = 8.3 Hz, 2H), 7.13 (s, 1H), 7.06 (d, *J* = 8.4 Hz, 1H), 5.69 (s, 1H), 4.89 (t, *J* = 6.6 Hz, 1H), 3.97 (t, *J* = 7.6 Hz, 1H), 3.81 (d, *J* = 11.1 Hz, 2H), 3.69 (d, *J* = 10.9 Hz, 2H), 2.37 (s, 3H), 2.24 – 2.06 (m, 1H), 2.05 – 1.92 (m, 2H), 1.92 – 1.78 (m, 1H), 1.78 – 1.59 (m, 2H), 1.55 – 1.43 (m, 2H), 1.39 – 1.12 (m, 19H), 1.10 – 0.94 (m, 4H), 0.92 – 0.74 (m, 15H). ^{13}C NMR (101 MHz, $CDCl_3$) δ 154.16, 152.84, 149.72, 149.37, 149.34, 149.30, 148.34, 143.87, 142.57, 142.50, 142.43, 142.12, 142.08, 142.04, 140.67, 140.65, 140.63, 140.22, 135.35, 132.67, 131.61, 130.13, 130.09, 130.05, 129.81, 128.76, 127.95, 127.33, 126.32, 125.48, 125.35, 125.27, 120.25, 107.47, 98.45, 69.29, 45.47, 35.96, 35.90, 35.71, 35.64, 35.20, 33.77, 30.25, 28.96, 28.88, 28.86, 24.49, 23.07, 23.02, 23.01, 21.89, 20.84, 17.79, 17.73, 17.69, 17.63, 14.23, 14.20, 10.82, 10.81. (More peaks than expected are observed due to the mixture of isomers.) HRMS (MALDI) *m/z*: $[M]^+$ calcd. for $C_{54}H_{67}N_3O_2S_3Si$: 913.4165; found, 914.4054. Anal. Calcd. for $C_{54}H_{67}N_3O_2S_3Si$: C, 70.93; H, 7.39; N, 4.60. Found: C, 70.91; H, 7.34; N, 4.47.

*7-(8-(6-(5,5-dimethyl-1,3-dioxan-2-yl)-4,4-bis(2-ethylhexyl)-4H-silolo[3,2-b:4,5-b']dithiophen-2-yl)-2,3-bis(4-(dodecyloxy) phenyl)pyrido[3,4-b]pyrazin-5-yl)-4-(p-tolyl)-1,2,3,3a,4,8b-hexahydrocyclopenta[b]indole (**7b**):* Compound **5b** (489.1 mg, 0.5 mmol), compound **6** (658.9 mg, 1.0 mmol), [1,1'bis(diphenyl phosphino)ferrocene]dichloro-palladium(II) (36.6 mg, 0.05 mmol) and potassium carbonate (345 mg, 2.5 mmol) were placed in a dry two-neck round bottom flask. Under nitrogen, methanol (5.0 mL) and anhydrous toluene (20 mL) were added and the reaction mixture was subjected to three freeze/pump/thaw cycles after which the reaction flask was refilled with nitrogen. The solution was heated to 80 °C for 12 hours. The solvents were removed under reduced pressure and the raw product was extracted using DCM and water. The DCM extract was filtered through Celite® and then passed through a column of silica eluting with hexanes /dichloromethane (volume = 4:3) to get purple solid (579 mg, yield: 81%). ^{1}H NMR (400 MHz, $CDCl_3$) δ 9.17 (s, 1H), 8.23 (s, 1H), 8.18 (d, *J* = 8.5 Hz, 1H), 7.83 (d, *J* = 8.6 Hz, 2H), 7.80 (s, 1H), 7.68 (d, *J* = 8.7 Hz, 2H), 7.29 (d, *J* = 8.3 Hz, 2H), 7.22 (d, *J* = 8.3 Hz, 2H), 7.14 (s, 1H), 7.07 (d, *J* = 8.5 Hz, 1H), 6.97 (d, *J* = 8.8 Hz, 2H), 6.89 (d, *J* = 8.7 Hz, 2H), 5.71 (s, 1H), 4.91 (t, *J* = 6.6 Hz, 1H), 4.07 (t, *J* = 6.6 Hz, 2H), 4.03 – 3.94 (m, 3H), 3.83 (d, *J* = 11.0 Hz, 2H), 3.71 (d, *J* = 11.0 Hz, 2H), 2.39 (s, 3H), 2.26 – 2.05 (m, 2H), 2.05 – 1.92 (m, 1H), 1.93 – 1.76 (m, 5H), 1.76 – 1.61 (m, 2H), 1.59 – 1.44 (m, 6H), 1.39 – 1.13 (m, 48H), 1.09 – 0.96 (m, 4H), 0.95 – 0.69 (m, 24H). ^{13}C NMR (101 MHz, $CDCl_3$) δ 160.64, 160.12, 156.40, 154.03, 152.51, 152.47, 152.43, 151.88, 149.76, 149.73, 149.70, 149.24, 142.95, 142.41,

142.34, 142.28, 142.27, 142.22, 142.16, 141.69, 141.66, 141.64, 140.10, 139.48, 137.33, 137.30, 137.27, 134.63, 133.20, 132.03, 131.75, 131.73, 131.43, 131.22, 130.52, 129.84, 128.66, 128.63, 128.59, 128.01, 127.81, 123.98, 120.53, 114.43, 114.34, 106.93, 98.66, 69.34, 68.20, 68.11, 45.47, 35.97, 35.93, 35.74, 35.67, 35.20, 33.73, 31.98, 30.27, 29.75, 29.72, 29.70, 29.70, 29.66, 29.64, 29.50, 29.47, 29.41, 29.34, 29.28, 28.93, 28.91, 26.11, 26.10, 24.53, 23.10, 23.05, 22.75, 21.92, 20.88, 17.78, 14.25, 14.23, 14.19, 10.86. (More peaks than expected are observed due to the mixture of isomers.) HRMS (MALDI) *m/z*: $[M]^+$ calcd. for $C_{91}H_{124}N_4O_4S_2Si$: 1428.8833; found, 1429.8869. Anal. Calcd. for $C_{91}H_{124}N_4O_4S_2Si$: C, 76.42; H, 8.74; N, 3.92. Found: C, 76.12; H, 8.85; N, 3.75.

*13-(6-(5,5-dimethyl-1,3-dioxan-2-yl)-4,4-bis(2-ethylhexyl)-4H-silolo[3,2-b:4,5-b']dithiophen-2-yl)-3,6-didodecyl-10-(4-(p-tolyl)-1,2,3,3a,4,8b-hexahydrocyclopenta[b]indol-7-yl)dibenzo[f,h]pyrido[3,4-b]quinoxaline (**7c**):* Compound **5c** (600.0 mg, 0.64 mmol), compound **6** (836.8 mg, 1.27 mmol), [1,1'bis(diphenylphosphino)ferrocene]dichloropalladium(II) (46.5 mg, 0.06 mmol) and potassium carbonate (439.5 mg, 3.18 mmol) were placed in a dry two-neck round bottom flask. Under nitrogen, methanol (7.0 mL) and anhydrous toluene (28 mL) were added and the reaction mixture was subjected to three freeze/pump/thaw cycles after which the reaction flask was refilled with nitrogen. The solution was heated to 80 °C for 12 hours. The solvents were removed under reduced pressure and the crude product was extracted using DCM and water. The DCM extract was filtered through Celite® and then passed through a column of silica eluting with hexanes/DCM (volume = 2:1) to get dark green solid (532 mg, yield: 60%). ^{1}H NMR (400 MHz, $CDCl_3$) δ 9.50 (d, *J* = 8.2 Hz, 1H), 9.29 (s, 1H), 9.16 (d, *J* = 8.2 Hz, 1H), 8.42 – 8.27 (m, 4H), 7.89 (s, 1H), 7.75 (d, *J* = 8.3 Hz, 1H), 7.56 (d, *J* = 8.3 Hz, 1H), 7.35 (d, *J* = 8.4 Hz, 2H), 7.25 (d, *J* = 8.3 Hz, 2H), 7.20 – 7.12 (m, 2H), 5.75 (s, 1H), 5.06 – 4.86 (m, 1H), 4.16 – 3.98 (m, 1H), 3.86 (d, *J* = 11.1 Hz, 2H), 3.73 (d, *J* = 11.0 Hz, 2H), 2.95 (2t, *J* = 7.7, 7.7 Hz, 4H), 2.41 (s, 1H), 2.27 – 2.14 (m, 2H), 2.11 – 1.98 (m, 1H), 1.97 – 1.68 (m, 7H), 1.63 – 1.10 (m, 54H), 1.16 – 0.97 (m, 4H), 0.96 – 0.69 (m, 24H). ^{13}C NMR (101 MHz, $CDCl_3$) δ 157.18, 152.61, 152.58, 152.54, 149.86, 149.16, 146.52, 145.68, 144.01, 142.46, 142.39, 142.33, 142.20, 142.10, 141.78, 141.75, 141.72, 140.57, 140.12, 137.61, 134.74, 134.58, 132.92, 132.09, 132.01, 131.65, 129.86, 128.97, 128.51, 128.31, 128.18, 128.06, 127.98, 127.84, 126.71, 124.07, 122.48, 122.42, 120.43, 107.03, 98.74, 83.97, 69.37, 45.56, 36.86, 36.67, 36.04, 36.01, 35.82, 35.75, 35.21, 33.83, 31.99, 31.68, 30.32, 29.81, 29.78, 29.73, 29.68, 29.65, 29.57, 29.44, 29.00, 28.97, 28.95, 24.80, 24.61, 23.16, 23.10, 22.76, 21.96, 20.91, 17.86, 14.29, 14.27, 14.19, 10.92. (More peaks than expected are observed due to the mixture of isomers.) HRMS (MALDI) *m/z*: $[M]^+$ calcd. for $C_{91}H_{122}N_4O_2S_2Si$: 1395.8857; found, 1395.8927. Anal. Calcd. for $C_{91}H_{122}N_4O_2S_2Si$: C, 78.28; H, 8.81; N, 4.01. Found: C, 78.29; H, 8.69; N, 3.87.

*4,4-bis(2-ethylhexyl)-6-(7-(4-(p-tolyl)-1,2,3,3a,4,8b-hexahydrocyclopenta[b]indol-7-yl)benzo[c][1,2,5]thiadiazol-4-yl)-4H-silolo[3,2-b:4,5-b']dithiophene-2-carbaldehyde (**8a**):* Compound **7a** (230 mg, 0.25 mmol) was dissolved in tetrahydrofuran (10.0 mL) and stirred at room temperature for 5 minutes. Water (2.5 mL) was added and reaction was stirred for another 5 minutes. Trifluoroacetic acid (0.39 mL, 5.03 mmol) was added and the reaction was stirred at room temperature for 12 hours under nitrogen atmosphere. Saturated sodium bicarbonate solution (40.0 mL) was added and reaction mixture stirred for an additional hour at room temperature. The organic layer was extracted from dichloromethane (40 x 3 mL), dried over anhydrous sodium sulfate and solvent removed to get the crude product which was passed through a column of silica eluting with hexanes /dichloromethane (volume = 1:1) to get a purple solid (155 mg, yield: 75%). ^{1}H NMR (400 MHz, $CDCl_3$) δ 9.92 (s, 1H), 8.18 (t, *J* = 4.0 Hz, 1H), 7.96 (d, *J* = 7.6 Hz, 1H), 7.82 (s, 1H), 7.80 – 7.74 (m, 2H), 7.71 (d, *J* = 7.6 Hz, 1H), 7.27 (d, *J* = 8.5 Hz, 2H), 7.21 (d, *J* = 8.3 Hz, 2H), 7.06 (d, *J* = 8.4 Hz, 1H), 4.97 – 4.78 (m, 1H), 3.97 (td, *J* = 8.7, 2.1 Hz, 1H), 2.38 (s, 3H), 2.20 – 2.05 (m, 1H), 2.05 – 1.93 (m, 2H), 1.91 – 1.78 (m, 1H), 1.78 – 1.57 (m, 2H), 1.55 – 1.44 (m, 2H), 1.39 – 1.17 (m, 16H), 1.12 – 1.04 (m, 4H), 0.91 – 0.78 (m, 12H). ^{13}C NMR (101 MHz, $CDCl_3$) δ 182.65, 158.52, 158.49, 158.46, 154.08, 152.77, 148.63, 148.43, 148.39, 148.36, 148.20, 144.71, 144.36, 143.77, 143.68, 143.59, 140.06, 139.74, 135.43, 133.77, 131.81, 129.84, 128.93, 126.99, 126.18, 126.06, 125.54, 124.40, 120.40, 107.43, 69.33, 45.44, 35.94, 35.93, 35.72, 35.70, 35.24, 33.72, 28.93, 28.90, 24.47, 23.01, 22.98, 20.85, 17.63, 17.59, 17.54, 17.49, 14.18, 14.16, 10.83, 10.82. (More peaks than expected are observed due to the mixture of isomers.) HRMS (MALDI) *m/z*: $[M]^+$ calcd. for $C_{49}H_{57}N_3OS_3Si$: 827.3433; found, 827.3409. Anal. Calcd. for $C_{49}H_{57}N_3OS_3Si$: C, 71.05; H, 6.94; N, 5.07. Found: C, 70.90; H, 6.87; N, 4.98.

*6-(2,3-bis(4-(dodecyloxy)phenyl)-5-(4-(p-tolyl)-1,2,3,3a,4,8b-hexahydrocyclopenta[b]indol-7-yl)pyrido[3,4-b]pyrazin-8-yl)-4,4-bis(2-ethylhexyl)-4H-silolo[3,2-b:4,5-b']dithiophene-2-carbaldehyde (**8b**):* Compound **7b** (300 mg, 0.2 mmol) was dissolved in tetrahydrofuran (8.0 mL) and stirred at room temperature for 5 minutes. Water (2.0 mL) was added and reaction was stirred for another 5 minutes. Trifluoroacetic acid (0.32 mL, 4.2 mmol) was added and the reaction was stirred at room temperature for 12 hours under nitrogen atmosphere. Saturated sodium bicarbonate solution (40.0 mL) was added and reaction mixture stirred for an additional hour at room temperature. The organic layer was extracted from dichloromethane (40 x 3 mL), dried over anhydrous sodium sulfate and solvent removed to get the crude product which was passed through a column of silica eluting with hexanes /dichloromethane (volume = 5:3) to get a purple solid (161 mg, yield: 60%). ^{1}H NMR (400 MHz, $CDCl_3$) δ 9.91 (s, 1H), 9.21 (s, 1H), 8.24 (s, 1H), 8.20 (d, *J* = 8.5 Hz, 1H), 7.86 (s, 1H), 7.83 (d, *J* = 8.7 Hz, 2H), 7.75 (s, 1H), 7.67 (d, *J* = 8.8 Hz, 2H), 7.27 (d, *J* = 9.5 Hz, 2H), 7.21 (d, *J* = 8.4 Hz, 2H), 7.05 (d, *J* = 8.5 Hz, 1H), 6.97 (d, *J* = 8.8 Hz, 2H), 6.88 (d, *J* = 8.8 Hz, 2H), 5.01 – 4.78 (m, 1H), 4.07 (t, *J* = 6.5 Hz, 2H), 4.03 – 3.86 (m, 3H), 2.37 (s, 3H), 2.23 – 2.02 (m,

2H), 2.02 – 1.90 (m, 1H), 1.90 – 1.75 (m, 5H), 1.75 – 1.58 (m, 2H), 1.58 – 1.44 (m, 6H), 1.42 – 1.12 (m, 48H), 1.12 – 1.01 (m, 4H), 0.96 – 0.75 (m, 18H). ^{13}C NMR (101 MHz, $CDCl_3$) δ 182.74, 160.87, 160.21, 159.05, 159.03, 159.02, 157.20, 154.34, 152.16, 150.88, 150.85, 150.82, 149.54, 146.82, 146.74, 146.67, 144.45, 143.64, 143.55, 143.47, 143.08, 141.17, 141.16, 141.14, 139.94, 139.47, 134.70, 133.22, 132.01, 131.97, 131.94, 131.42, 131.00, 130.28, 129.86, 128.26, 128.23 , 128.21, 127.88, 127.76, 123.05, 120.70, 114.45, 114.37, 106.89, 69.39, 68.27, 68.13, 45.42, 35.93, 35.72, 35.21, 33.67, 31.95, 29.72, 29.70, 29.67, 29.64, 29.62, 29.50, 29.45, 29.39, 29.39, 29.33, 29.25, 28.93, 28.89, 26.11, 26.07, 24.50, 23.02, 22.99, 22.73, 20.88, 17.63, 14.18, 14.16, 10.85, 10.83. (More peaks than expected are observed due to the mixture of isomers.) HRMS (MALDI) *m/z*: $[M]^+$ calcd. for $C_{86}H_{114}N_4O_3S_2Si$: 1342.8102; found, 1342.8122. Anal. Calcd. for $C_{91}H_{124}N_4O_4S_2Si$: C, 76.85; H, 8.55; N, 4.17. Found: C, 77.03; H, 8.60; N, 4.11.

*6-(3,6-didodecyl-10-(4-(p-tolyl)-1,2,3,3a,4,8b-hexahydrocyclopenta[b]indol-7-yl)dibenzo[f,h]pyrido[3,4-b]quinoxalin-13-yl)-4,4-bis(2-ethylhexyl)-4H-silolo[3,2-b:4,5-b']dithiophene-2-carbaldehyde (**8c**):* Compound **7c** (532.0 mg, 0.38 mmol) was dissolved in tetrahydrofuran (15.0 mL) and stirred at room temperature for 5 minutes. Water (3.8 mL) was added and reaction was stirred for another 5 minutes. Trifluoroacetic acid (0.59 mL, 7.6 mmol) was added, and the reaction was stirred at room temperature for 12 hours under nitrogen atmosphere. Saturated sodium bicarbonate solution (50.0 mL) was added and reaction mixture stirred for an additional hour at room temperature. The organic layer was extracted from dichloromethane (40 x 3 mL), dried over anhydrous sodium sulfate and solvent removed to get the crude product which was passed through a column of silica eluting with hexanes /dichloromethane (volume = 2:1) to get a dark green solid (204 mg, yield: 41%). ^{1}H NMR (400 MHz, $CDCl_3$) δ 9.97 (s, 1H), 9.38 (d, *J* = 6.5 Hz, 1H), 9.29 (s, 1H), 9.03 (d, *J* = 6.5 Hz, 1H), 8.44 – 8.32 (m, 2H), 8.26 (d, *J* = 7.7 Hz, 2H), 7.93 (s, 1H), 7.81 (s, 1H), 7.67 (d, *J* = 7.7 Hz, 1H), 7.48 (d, *J* = 7.9 Hz, 1H), 7.34 (d, *J* = 8.4 Hz, 2H), 7.26 (d, *J* = 8.4 Hz, 2H), 7.13 (d, *J* = 8.4 Hz, 1H), 4.97 (t, *J* = 6.6 Hz, 1H), 4.09 – 3.87 (m, 1H), 2.91 (2t, *J* = 7.6, 7.6 Hz, 4H), 2.42 (s, 3H), 2.25 – 2.13 (m, 2H), 2.08 – 1.96 (m, 1H), 1.95 – 1.66 (m, 7H), 1.66 – 1.18 (m, 54H), 1.14 (d, *J* = 6.7 Hz, 4H), 0.99 – 0.79 (m, 18H). ^{13}C NMR (101 MHz, $CDCl_3$) δ 182.62, 159.20, 157.61, 150.87, 150.85, 150.82, 149.33, 146.67, 145.59, 144.48, 143.83, 143.56, 143.51, 142.41, 142.26, 142.12, 141.38, 140.46, 140.23, 139.95, 134.56, 132.84, 132.81, 132.25, 131.93, 131.76, 129.87, 128.72, 128.59, 128.37, 128.27, 128.11, 127.95, 127.47, 126.59, 122.91, 122.35, 120.64, 120.53, 106.91, 69.36, 45.51, 36.88, 36.70, 36.02, 35.82, 35.26, 33.77, 31.99, 31.70, 29.75, 29.44, 28.99, 28.96, 24.61, 23.11, 23.09, 22.75, 20.93, 17.68, 14.25, 14.18, 10.91. (More peaks than expected are observed due to the mixture of isomers.) HRMS (MALDI) *m/z*: $[M]^+$ calcd. for $C_{86}H_{112}N_4OS_2Si$: 1308.8047; found, 1308.7982. Anal. Calcd. for $C_{86}H_{112}N_4OS_2Si$: C, 78.85; H, 8.62; N, 4.28. Found: C, 78.88; H, 8.53; N, 4.36.

*(E)-3-(4,4-bis(2-ethylhexyl)-6-(7-(4-(p-tolyl)-1,2,3,3a,4,8b-hexahydrocyclopenta[b]indol-7-yl)benzo[c][1,2,5]thiadiazol-4-yl)-4H-silolo[3,2-b:4,5-b']dithiophen-2-yl)-2-cyanoacrylic acid (**B-87**):* Compound **8a** (200.0 mg, 0.24 mmol), and cyanoacetic acid (786.0 mg, 18.5 mmol) were placed in a dry two-neck round bottom flask with reflux condenser attached. Under nitrogen, anhydrous chloroform (16 mL), anhydrous acetonitrile (16 mL) and piperidine (912 µL, 9.24 mmol) were added and the solution heated to reflux at 65°C for 12 hours. The solvent was removed under reduced pressure and the crude mixture passed through a column of silica eluting with dichloromethane/methanol (volume = 25:1) to give a dark purple powder (120 mg, 56%). ^{1}H NMR (400 MHz, $CDCl_3$) δ 8.40 (s, 1H), 8.21 (t, *J* = 3.1 Hz, 1H), 7.94 – 7.59 (m, 5H), 7.27 (d, *J* = 8.2 Hz, 2H), 7.20 (d, *J* = 8.2 Hz, 2H), 7.04 (d, *J* = 8.3 Hz, 1H), 4.89 (t, *J* = 7.1 Hz, 1H), 3.96 (t, *J* = 8.1 Hz, 1H), 2.38 (s, 3H), 2.22 – 2.04 (m, 1H), 2.04 – 1.92 (m, 2H), 1.92 – 1.78 (m, 1H), 1.78 – 1.46 (m, 4H), 1.45 – 1.19 (m, 16H), 1.12 (s, 4H), 0.99 – 0.78 (m, 12H). ^{13}C NMR (101 MHz, $CDCl_3$) δ 169.00, 161.20, 153.93, 152.63, 149.72, 148.62, 147.86, 145.88, 144.61, 142.64, 140.04, 137.38, 135.42, 133.84, 131.79, 130.12, 129.84, 128.98, 126.92, 126.24, 125.89, 125.54, 124.11, 124.06, 120.37, 116.46, 107.42, 93.78, 69.32, 45.43, 35.95, 35.75, 35.24, 33.72, 28.91, 24.48, 23.04, 23.00, 20.85, 17.65, 17.60, 17.51, 17.45, 14.19, 10.83. HRMS (MALDI) *m/z*: $[M]^+$ calcd. for $C_{52}H_{58}N_4O_2S_3Si$: 894.3491; found, 894.3494. Anal. Calcd. for $C_{52}H_{58}N_4O_2S_3Si$: C, 69.76; H, 6.53; N, 6.26. Found: C, 69.67; H, 6.56; N, 6.21.

*(E)-3-(6-(2,3-bis(4-(dodecyloxy)phenyl)-5-(4-(p-tolyl)-1,2,3,3a,4,8b-hexahydrocyclopenta[b]indol-7-yl)pyrido[3,4-b]pyrazin-8-yl)-4,4-bis(2-ethylhexyl)-4H-silolo[3,2-b:4,5-b']dithiophen-2-yl)-2-cyanoacrylic acid (**Q-85**):* Compound **8b** (138.0 mg, 0.10 mmol), and cyanoacetic acid (672.0 mg, 7.80 mmol) were placed in a dry two-neck round bottom flask with reflux condenser attached. Under nitrogen, anhydrous chloroform (16 mL), anhydrous acetonitrile (16 mL) and piperidine (381 µL, 3.87 mmol) were added and the solution heated to reflux at 65°C for 12 hours. The solvent was removed under reduced pressure and the crude mixture passed through a column of silica eluting with dichloromethane/methanol (volume = 30:1) to give a dark purple powder (110 mg, 78%). ^{1}H NMR (400 MHz, $CDCl_3$) δ 9.23 (s, 1H), 8.40 (s, 1H), 8.20 (s, 1H), 8.16 (d, *J* = 8.7 Hz, 1H), 7.93 (s, 1H), 7.83 (d, *J* = 8.6 Hz, 2H), 7.80 (s, 1H), 7.68 (d, *J* = 8.7 Hz, 2H), 7.30 (d, *J* = 8.5 Hz, 2H), 7.23 (d, *J* = 8.5 Hz, 2H), 7.06 (d, *J* = 8.5 Hz, 1H), 7.00 (d, *J* = 8.8 Hz, 2H), 6.90 (d, *J* = 8.8 Hz, 2H), 5.07 – 4.84 (m, 1H), 4.07 (t, *J* = 6.3 Hz, 2H), 4.03 – 3.93 (m, 3H), 2.39 (s, 3H), 2.31 – 2.07 (m, 2H), 2.07 – 1.90 (m, 1H), 1.90 – 1.78 (m, 5H), 1.76 – 1.63 (m, 2H), 1.59 – 1.43 (m, 6H), 1.44 – 1.16 (m, 48H), 1.10 (d, 4H), 0.95 – 0.77 (m, 18H). ^{13}C NMR (101 MHz, $CDCl_3$) δ 167.56, 161.02, 160.32, 160.04, 156.88, 155.02, 152.65, 151.02, 150.05, 147.62, 147.53, 147.44, 146.72, 144.67, 144.55, 144.45, 141.95, 141.49, 141.20, 140.00, 139.69, 137.48, 134.87, 133.43, 132.51, 132.27, 132.01, 131.46, 130.80, 130.07, 129.89, 129.24, 128.11, 126.15, 123.75, 120.98, 117.26, 114.56, 114.39, 106.80, 96.17, 69.49, 68.24, 68.15, 45.36, 35.89, 35.72, 35.70, 35.26, 33.60, 31.94, 29.70, 29.69, 29.66, 29.62, 29.61, 29.48, 29.44,

29.37, 29.28, 29.24, 28.90, 28.88, 28.86, 26.11, 26.06, 24.50, 23.00, 22.98, 22.71, 20.89, 17.63, 14.17, 14.15, 10.81, 10.80. (More peaks than expected are observed due to the mixture of isomers.) HRMS (MALDI) *m/z*: $[M]^+$ calcd. for $C_{89}H_{115}N_5O_4S_2Si$: 1409.8160; found, 1409.8121. Anal. Calcd. for $C_{91}H_{124}N_4O_4S_2Si$: C, 75.75; H, 8.21; N, 4.96. Found: C, 75.69; H, 8.17; N, 5.04.

*(E)-2-cyano-3-(6-(3,6-didodecyl-10-(4-(p-tolyl)-1,2,3,3a,4,8b-hexahydrocyclopenta[b]indol-7-yl)dibenzo[f,h]pyrido[3,4-b] quinoxalin-13-yl)-4,4-bis(2-ethylhexyl)-4H-silolo[3,2-b:4,5-b']dithiophen-2-yl)acrylic acid (**Q-93**):* Compound **8c** (204.0 mg, 0.16 mmol), and cyanoacetic acid (1019.7 mg, 12.0 mmol) were placed in a dry two-neck round bottom flask with reflux condenser attached. Under nitrogen, anhydrous chloroform (20 mL), anhydrous acetonitrile (20 mL) and piperidine (592 µL, 5.99 mmol) were added and the solution heated to reflux at 65 °C for 12 hours. The solvent was removed under reduced pressure and the crude mixture passed through a column of silica eluting with dichloromethane/methanol (volume = 40:1) to give a dark green powder (150 mg, yield: 70%). ^{1}H NMR (400 MHz, $CDCl_3$) δ 9.34 (s, 1H), 9.26 (s, 1H), 9.02 (s, 1H), 8.45 (s, 1H), 8.28 (s, 4H), 7.94 (d, *J* = 25.3 Hz, 2H), 7.71 (s, 1H), 7.48 (s, 1H), 7.34 (d, *J* = 7.9 Hz, 2H), 7.25 (d, *J* = 8.1 Hz, 2H), 7.13 (d, *J* = 8.4 Hz, 1H), 4.98 (s, 1H), 4.02 (s, 1H), 2.91 (s, 4H), 2.41 (s, 3H), 2.21 (s, 2H), 2.02 (s, 1H), 1.81 (s, 7H), 1.65 – 1.04 (m, 58H), 0.94 – 0.78 (m, 18H). ^{13}C NMR (101 MHz, $CDCl_3$) δ 167.64, 160.00, 157.70, 150.95, 149.93, 147.52, 147.19, 146.63, 146.05, 144.62, 142.77, 141.73, 140.94, 139.74, 137.55, 137.53, 134.85, 134.77, 133.14, 132.86, 132.32, 132.18, 130.16, 129.92, 129.33, 128.64, 128.51, 128.38, 128.27, 127.81, 127.54, 126.85, 123.76, 122.52, 120.85, 117.30, 106.87, 69.47, 45.43, 36.84, 36.72, 35.94, 35.78, 35.26, 33.69, 31.94, 31.71, 31.68, 29.73, 29.68, 29.62, 29.58, 29.38, 28.93, 24.58, 23.05, 23.02, 22.70, 20.91, 17.65, 14.19, 14.13, 10.86. HRMS (MALDI) *m/z*: $[M+H]^+$ calcd. for $C_{89}H_{113}N_5O_2S_2Si$: 1376.8183; found, 1376.8198. Anal. Calcd. for $C_{89}H_{113}N_5O_2S_2Si$: C, 77.62; H, 8.27; N, 5.09. Found: C, 77.73; H, 8.22; N, 5.12.

Fabrication of DSSCs. The photoelectrode was fabricated by repeating screen printing process with commercial colloidal paste (Dyesol 18NR-T) layer (12 µm) and scattering layer (4 µm), respectively. Afterwards, the TiO_2 films were heated gradually under an air flow at 325 °C for 5 min, 375 °C for 5 min, 450 °C for 15 min, and 500 °C for 15 min. Prior to dye adsorption, the TiO_2 films were post treated by 0.04 M $TiCl_4$ solution to increase the surface area and improve the connectivity of the nanoparticles. Subsequently, the photoanodes sintered once again and cooled to room temperature. Then they were immersed into a binary solvent system ($CHCl_3$:C_2H_5OH= 6:4) with sensitizers (3× 10^{-4} M), respectively. For the counter electrode, the H_2PtCl_6 in 2-propanol solution presented a uniform distribution on FTO glass by spin coating method, and the cathode was heated under 400 °C for deposition of platinum. Eventually, the two electrodes were sealed with thermoplastic Surlyn, and an electrolyte solution was injected through one hole in the counter electrode to finish the sandwiches type-solar cells. The electrolyte is composed of 1.0 M 1,3-dimethylimidazolium iodide, 0.03 M iodine, 0.1 M guanidinium thiocyanate, 0.5 M tert-butylpyridine, 0.05 M lithium iodide in acetonitrile:valeronitrile (85:15, v/v). The active area of all DSSCs is 0.12 cm^2.

Photovoltaic property measurements. The current-voltage photovoltaic characterization was performed using the setup consisting of a 450 W xenon lamp (Oriel), a Schott K113 Tempax sunlight filter (PräzisionsGlas & Optik GmbH), and a Keithley 2400 source meter which applies potential bias and measures the photogenerated current. Monochromatic incident photon-to-current conversion efficiency (IPCE) was obtained via the setup using a SR830 lock-in amplifier, a 300 W xenon lamp (ILC Technology) and a Gemini-180 double monochromator (Jobin-Yvon Ltd.). A Zahner IM6e Impedance Analyzer (ZAHNER-Elektrik GmbH & CoKG, Kronach, Germany) was employed to carry out the electrochemical impedance spectroscopy. The frequency range was 0.1 Hz-100 kHz and the applied bias was from -0.5 V to -0.80 V or from -0.55 V to -0.80 V with about 50 mV progressive increase under dark condition. The magnitude of the alternating signal was 5 mV, and the spectra was characterized with Z-View software. Dye-loading measurements were conducted by immersing dye-coated TiO_2 films with 0.1 M NaOH THF/H_2O (v/v = 1/1) solution for 2h to perform the dye desorption. The absorption spectra of desorbed dye solutions were measured and total dye-loading was determined from a plot of standard samples.

Acknowledgements

This work was supported by NSFC for Creative Research Groups (21421004), NSFC/China (21372082, 21572062, 2116110444 and 91233207), and the Programme of Introducing Talents of Discipline to Universities (B16017). Gao would like to thank the funding of the visiting program, which is supported by China Scholarship Council (CSC).

Notes and references

1 (a) B. O'regan and M. Grätzel, *Nature* 1991**, 353**, 737; (b) B. E. Hardin, H. J. Snaith and M. D. McGehee, *Nature Photon.* 2012**, 6**, 162; (c) P. Docampo, S. Guldin, T. Leijtens, N. K. Noel, U. Steiner and H. J. Snaith, *Adv. Mater.* 2014**, 26**, 4013; (d) C. Grätzel and S. M. Zakeeruddin, *Mater. Today* 2013**, 16**, 11.

2 (a) C.-Y. Chen, M. Wang, J.-Y. Li, N. Pootrakulchote, L. Alibabaei, C.-h. Ngoc-le, J.-D. Decoppet, J.-H. Tsai, C. Grätzel and C.-G. Wu, *ACS Nano* 2009**, 3**, 3103; (b) D. Kuang, C. Klein, S. Ito, J. E. Moser, R. Humphry‐Baker, N. Evans, F. Duriaux, C. Grätzel, S. M. Zakeeruddin and M. Grätzel, *Adv. Mater.* 2007**, 19**, 1133; (c) P. Wang, S. M. Zakeeruddin, J. E. Moser, M. K. Nazeeruddin, T. Sekiguchi and M. Grätzel, *Nat. Mater.* 2003**, 2**, 402. (d) M. K. Nazeeruddin, F. D. Angelis, S. Fantacci, A. Selloni, G. Viscardi, P. Liska, S. Ito, B. Takeru and M. Grätzel, *J. Am. Chem. Soc.* 2005, **127**, 16835. (e) L. Han, A. Islam, H. Chen, C. Malapaka, B. Chiranjeevi, S. Zhang, X. Yang and M. Yanagida, *Energy Environ. Sci.* 2012, **5**, 6057.

3 (a) T. Bessho, S. M. Zakeeruddin, C. Y. Yeh, E. W. G. Diau and M. Grätzel, *Angew. Chem. Int. Ed.* 2010**, 49**, 6646; (b) S. Mathew, A. Yella, P. Gao, R. Humphry-Baker, B. F. Curchod, N. Ashari-Astani, I. Tavernelli, U. Rothlisberger, M. K.

Nazeeruddin and M. Grätzel, *Nat. Chem.* 2014**, 6**, 242-247; (c) M. Urbani, M. Grätzel, M. K. Nazeeruddin and T. Torres, *Chem. Rev.* 2014**, 114**, 12330; (d) Y. Xie, Y. Tang, W. Wu, Y. Wang, J. Liu, X. Li, H. Tian and W. Zhu, *J. Am. Chem. Soc.* 2015**, 137**, 14055; (e) A. Yella, H.-W. Lee, H. N. Tsao, C. Yi, A. K. Chandiran, M. K. Nazeeruddin, E. W.-G. Diau, C.-Y. Yeh, S. M. Zakeeruddin and M. Grätzel, *Science* 2011**, 334**, 629-634; (f) A. Yella, C. L. Mai, S. M. Zakeeruddin, S. N. Chang, C. H. Hsieh, C. Y. Yeh and M. Grätzel, *Angew. Chem. Int. Ed.* 2014**, 126**, 3017.

4 (a) A. Mishra, M. K. Fischer, P. Bäuerle, *Angew. Chem. Int. Ed.* 2009**, 48**, 2474; (b) Y. Wu and W. Zhu, *Chem. Soc. Rev.* 2013**, 42**, 2039; (c) Y.-S. Yen, H.-H. Chou, Y.-C. Chen, C.-Y. Hsu and J. T. Lin, *J. Mater. Chem.* 2012**, 22**, 8734.

5 (a) S. Haid, M. Marszalek, A. Mishra, M. Wielopolski, J. Teuscher, J. E. Moser, R. Humphry‐Baker, S. M. Zakeeruddin, M. Grätzel and P. Bäuerle, *Adv. Funct. Mater.* 2012**, 22**, 1291; (b) Y. Hong, J.-Y. Liao, D. Cao, X. Zang, D.-B. Kuang, L. Wang, H. Meier and C.-Y. Su, *J. Org. Chem.* 2011**, 76**, 8015.

6 W. Zhu, Y. Wu, S. Wang, W. Li, X. Li, J. Chen, Z. Wang and H. Tian, *Adv. Funct. Mater.* 2011**, 21**, 756.

7 (a) D. DiáCenso, *Chem. Commun.* 2012**, 48**, 10724; (b) S. Qu, C. Qin, A. Islam, Y. Wu, W. Zhu, J. Hua, H. Tian and L. Han, *Chem. Commun.* 2012**, 48**, 6972; (c) S. Qu, W. Wu, J. Hua, C. Kong, Y. Long and H. Tian, *J. Phys. Chem. C* 2009**, 114**, 1343; (d) J.-H. Yum, T. W. Holcombe, Y. Kim, K. Rakstys, T. Moehl, J. Teuscher, J. H. Delcamp, M. K. Nazeeruddin and M. Grätzel, *Sci. Rep.* 2013**, 3**, 2446.

8 (a) J. He, F. Guo, X. Li, W. Wu, J. Yang and J. Hua, *Chem. Eur. J.* 2012**, 18**, 7903; (b) J. He, W. Wu, J. Hua, Y. Jiang, S. Qu, J. Li, Y. Long and H. Tian, *J. Mater. Chem.* 2011**, 21**, 6054.

9 W. Ying, F. Guo, J. Li, Q. Zhang, W. Wu, H. Tian and J. Hua, *ACS Appl. Mater. Interfaces* 2012**, 4**, 4215.

10 Y. Wu, M. Marszalek, S. M. Zakeeruddin, Q. Zhang, H. Tian, M. Grätzel and W. Zhu, *Energy Environ. Sci.* 2012**, 5**, 8261.

11 J. Mao, F. Guo, W. Ying, W. Wu, J. Li and J. Hua, *Chem. Asian J.* 2012**, 7**, 982.

12 (a) D. W. Chang, H. J. Lee, J. H. Kim, S. Y. Park, S.-M. Park, L. Dai and J.-B. Baek, *Org. Lett.* 2011**, 13**, 3880; (b) K. Pei, Y. Wu, A. Islam, Q. Zhang, L. Han, H. Tian and W. Zhu, *ACS Appl. Mater. Interfaces* 2013**, 5**, 4986; (c) K. Pei, Y. Wu, W. Wu, Q. Zhang, B. Chen, H. Tian and W. Zhu, *Chem. Eur. J.* 2012**, 18**, 8190.

13 Q. Chai, W. Li, J. Liu, Z. Geng, H. Tian and W. Zhu, *Sci. Rep.* 2015**, 5**, 11330.

14 (a) F. M. Jradi, X. Kang, D. O'Neil, G. Pajares, Y. A. Getmanenko, P. Szymanski, T. C. Parker, M. A. El-Sayed and S. R. Marder, *Chem. Mater.* 2015**, 27**, 2480; (b) F. M. Jradi, D. O'Neil, X. Kang, J. Wong, P. Szymanski, T. C. Parker, H. L. Anderson, M. A. El-Sayed and S. R. Marder, *Chem. Mater.* 2015**, 27**, 6305.

15 W. Ying, J. Yang, M. Wielopolski, T. Moehl, J.-E. Moser, P. Comte, J. Hua, S. M. Zakeeruddin, H. Tian and M. Grätzel, *Chem. Sci.* 2014**, 5**, 206.

16 (a) M. Wang, S. Shi, D. Ma, K. Shi, C. Gao, L. Wang, G. Yu, Y. Li, X. Li and H. Wang, *Chem. Asian J.* 2014**, 9**, 2961; (b) X. Wang, Y. Zhou, T. Lei, N. Hu, E.-Q. Chen and J. Pei, *Chem. Mater.* 2010**, 22**, 3735.

17 A. Hagfeldt, G. Boschloo, L. Sun, L. Kloo, H. Pettersson, *Chem. Rev.* 2010**, 110**, 6595.

18 (a) A. Hagfeldt and M. Grätzel, *Chem. Rev.* 1995**, 95**, 49; (b) K. Kalyanasundaram and M. Grätzel, *Coord. Chem. Rev.* 1998**, 177**, 347.

19 N. G. Connelly and W. E. Geiger, *Chem. Rev.* 1996**, 96**, 877.

20 L.-L. Li and E. W.-G. Diau, *Chem. Soc. Rev.* 2013**, 42**, 291.

21 (a) J. Bisquert, I. Mora-Sero and F. Fabregat-Santiago, *ChemElectroChem* 2014**, 1**, 289; (b) F. Fabregat-Santiago, J. Bisquert, G. Garcia-Belmonte, G. Boschloo and A. Hagfeldt, *Sol. Energy Mater. Sol. Cells* 2005**, 87**, 117; (c) F. Fabregat-Santiago, G. Garcia-Belmonte, I. Mora-Seró and J. Bisquert, *Phys. Chem. Chem. Phys.* 2011**, 13**, 9083.

22 Y. Ooyama and Y. Harima, *ChemPhysChem* 2012**, 13**, 4032.

23 M. Wang, P. Chen, R. Humphry-Baker, S. M. Zakeeruddin and M. Grätzel, *ChemPhysChem* 2009**, 10**, 290.

24 H. N. Tsao, P. Comte, C. Yi and M. Grätzel, *ChemPhysChem* 2012**, 13**, 2976.

25 A. J. Frank, N. Kopidakis and J. van de Lagemaat, *Coord. Chem. Rev.* 2004**, 248**, 1165.

26 (a) Y. Hua, S. Chang, J. He, C. Zhang, J. Zhao, T. Chen, W. Y. Wong, W. K. Wong and X. Zhu, *Chem. Eur. J.* 2014**, 20**, 6300; (b) Y. Li, C. Chen, X. Sun, J. Dou and M. Wei, *ChemSusChem* 2014**, 7**, 2469.

27 D. Joly, L. Pellejà, S. Narbey, F. Oswald, J. Chiron, J. N. Clifford, E. Palomares and R. Demadrille, *Sci. Rep.* 2014**, 4**, 4033.

28 B.-L. Lee and T. Yamamoto, *Macromolecules* 1999**, 32**, 1375.

29 Y. Shirai, A. J. Osgood, Y. Zhao, Y. Yao, L. Saudan, H. Yang, C. Yu-Hung, L. B. Alemany, T. Sasaki and J.-F. Morin, *J. Am. Chem. Soc.* 2006**, 128**, 4854.

30 O. Miyata, N. Takeda, Y. Kimura, Y. Takemoto, N. Tohnai, M. Miyata and T. Naito, *Tetrahedron* 2006**, 62**, 3629.

Insert Table of Contents artwork here